

Supporting Information for

Mechanical Creep Instability of Nanocrystalline Methane Hydrates

Pinqiang Cao ^{1,*}, Jianlong Sheng ¹, Jianyang Wu ², Fulong Ning ³,

¹ School of Resource and Environmental Engineering, Wuhan University of Science and
Technology, Wuhan, Hubei 430081, China

² Department of Physics, Jiujiang Research Institute, Research Institute for Biomimetics and Soft
Matter, Fujian Provincial Key Laboratory for Soft Functional Materials Research, Xiamen
University, Xiamen 361005, China

³ Faculty of Engineering, China University of Geosciences, Wuhan, Hubei 430074, China

Email address:

Pinqiang Cao: pinqiang@wust.edu.cn;

Jianlong Sheng: shengjl@wust.edu.cn;

Jianyang Wu: jianyang@xmu.edu.cn;

Fulong Ning: nflzx@cug.edu.cn;

*To whom correspondence should be addressed: pinqiang@wust.edu.cn;

Supporting Figures

Figure S1

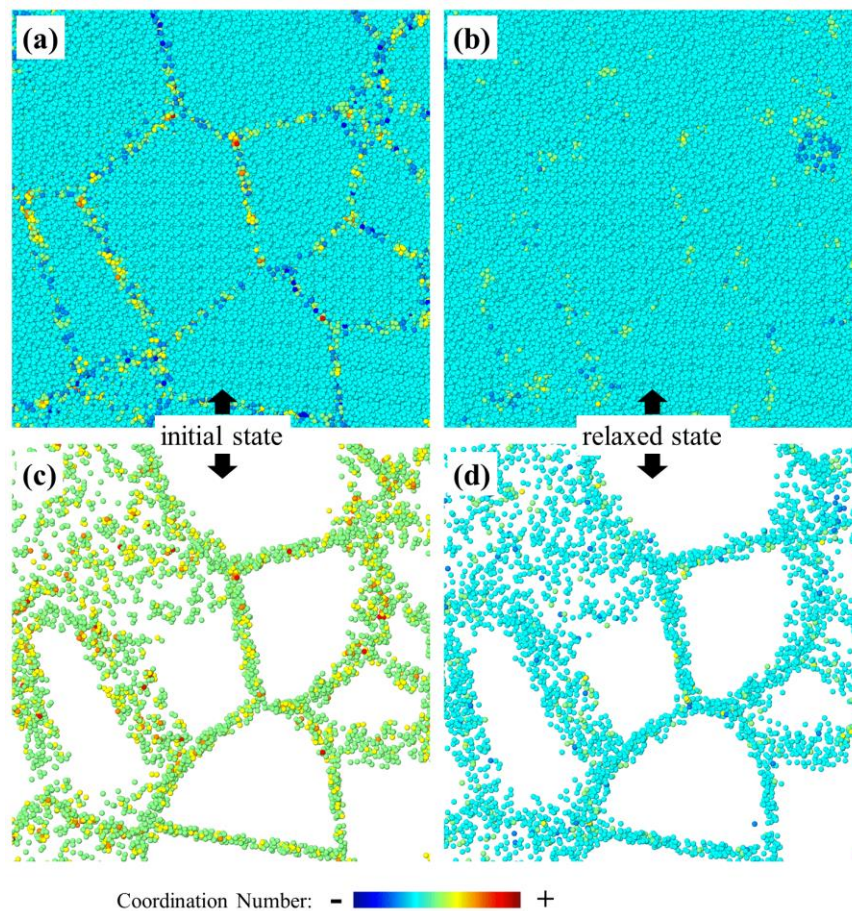


Figure S1. Localized structures captured from the polycrystals. (a) Localized structures captured from the polycrystal with an average grain size of about 10 nm at the initial state. (b) Localized structures captured from the polycrystal with an average grain size of about 10 nm at the relaxed state. (c) Localized grain boundary structures captured from the polycrystal with an average grain size of about 10 nm at the initial state. (d) Localized grain boundary structures captured from the polycrystal with an average grain size of about 10 nm at the relaxed state.

Water molecules in polycrystals are colored according to the coordination number of water particles in (a)-(d). Methane molecules are not shown for clarification in (a)-(d).

Figure S2

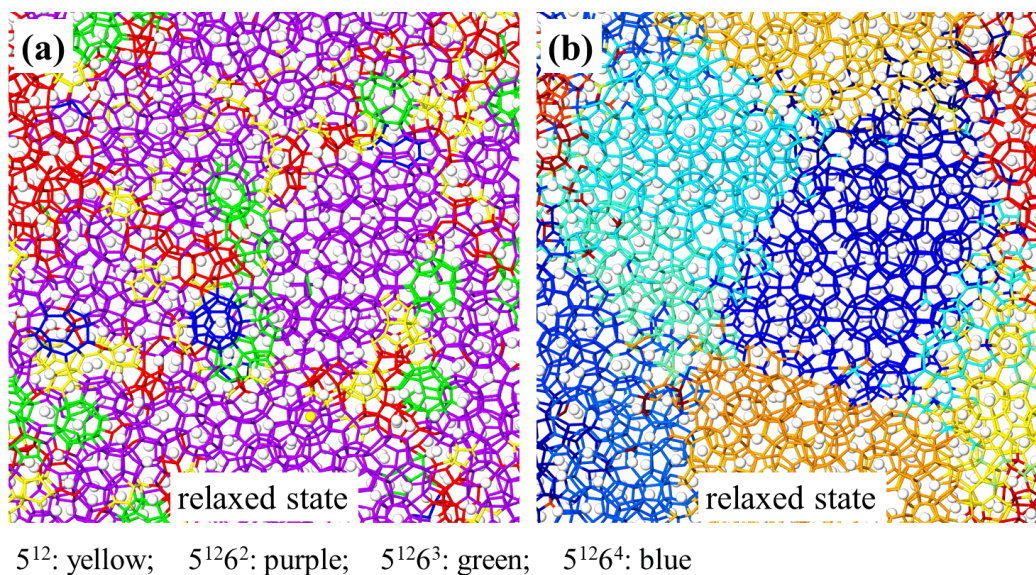


Figure S2. Localized water structures captured from the polycrystals. (a) Localized structures captured from the polycrystal with an average grain size of about 4 nm at the relaxed state. (b) Localized structures captured from the polycrystal with an average grain size of about 4 nm at the relaxed state. Water molecules in polycrystals are colored according to their cage-type in (a). The unidentified water molecules are colored with red at in (a). Crystalline grains in polycrystals are colored for clarification of grain morphology in (b). Methane molecules are colored with white in (a)-(b).

Figure S3

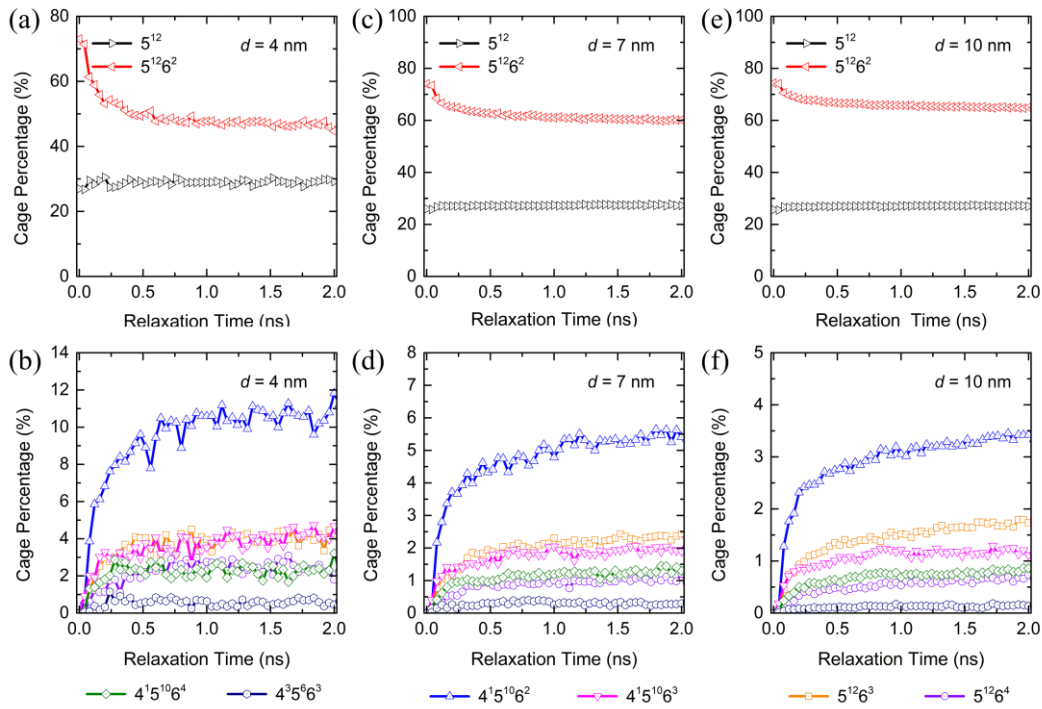


Figure S3. The percentages of identified water cages in nanocrystalline methane hydrates during MD relaxation processes. (a)-(b) nanocrystalline methane hydrates with an average grain size of 4 nm at 263.15 K and a confining pressure of 10 MPa. (c)-(d) nanocrystalline methane hydrates with an average grain size of 7 nm at 263.15 K and a confining pressure of 10 MPa. (e)-(f) nanocrystalline methane hydrates with an average grain size of 10 nm at 263.15 K and a confining pressure of 10 MPa. The percentage of cages for each type is obtained via dividing the number of each identified cage type by the total number of all identified cages in this work.

Figure S4

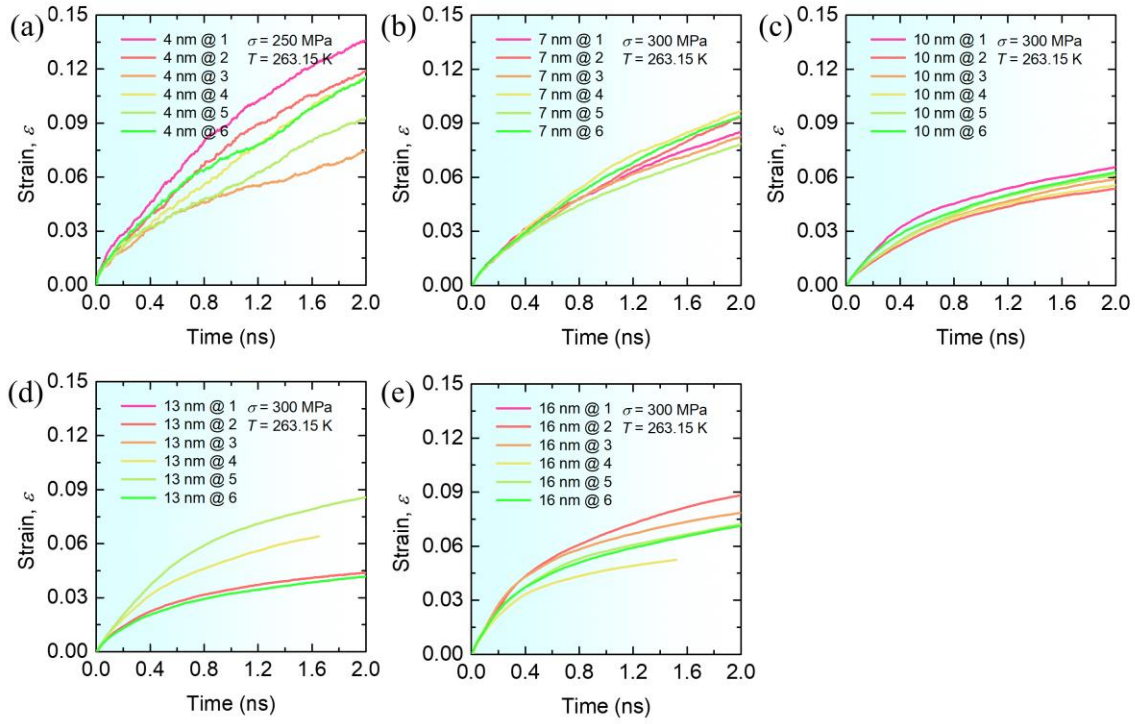


Figure S4. Creep behaviors of polycrystalline methane hydrates with different grain sizes.

Creep behaviors of polycrystalline methane hydrates with an average grain size of (a) 4 nm under a stress level of 250 MPa at a temperature of 263.15 K, (b) 7 nm under a stress level of 300 MPa at a temperature of 263.15 K, (c) 10 nm under a stress level of 300 MPa at a temperature of 263.15 K, (d) 13 nm under a stress level of 300 MPa at a temperature of 263.15 K, (e) 16 nm under a stress level of 300 MPa at a temperature of 263.15 K.

Figure S5

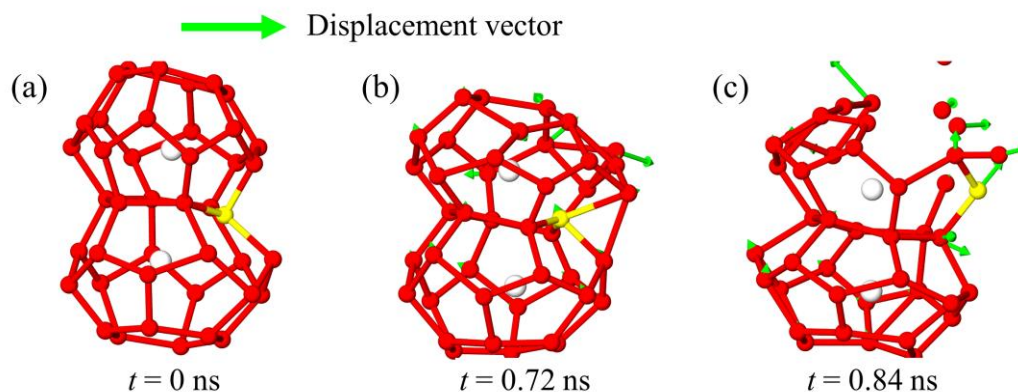


Figure S5. Typical localized snapshots of polycrystalline methane hydrates with an average grain size of 4 nm under a loading stress of 250 MPa at a temperature of 263.15 K. (a) creep time of 0 ns. (b) creep time of 0.72 ns. (c) creep time of 0.84 ns. The green arrow represents the displacement relative to the relaxed (equilibrium) state. The oxygen atoms which colored with yellow indicate that lattice diffusion occurs.

Table S1

Table S1. The initial dimension sizes of polycrystalline methane hydrate samples and the simulation boxes. Apparently, the dimension sizes of the simulation boxes are identical to those of the corresponding polycrystalline samples in our MD simulations.

Grain size (nm)	4 nm	7 nm	10 nm	13 nm	16 nm
Dimensions of the polycrystalline samples (nm ³)	9.3 × 9.3 × 9.3	16.3 × 16.3 × 16.3	23.2 × 23.2 × 23.2	30.2 × 30.2 × 30.2	37.2 × 37.2 × 37.2
Dimensions of the simulation boxes (nm ³)	9.3 × 9.3 × 9.3	16.3 × 16.3 × 16.3	23.2 × 23.2 × 23.2	30.2 × 30.2 × 30.2	37.2 × 37.2 × 37.2

Table S2

Table S2. Different stress exponents n for polycrystalline methane hydrates. The stress exponent n in the top five lines is estimated from our simulation results for polycrystalline methane hydrates at 263.15 K under different loading stresses (MPa). Both sixth and seventh lines contain extrapolated experimental estimates at about 260-287 K for polycrystalline methane hydrates from previous studies [1, 2](#).

Grain size (nm/ μ m)	4 (nm)	7 (nm)	10 (nm)	~ 20-40 (μ m)
100-150 (MPa)	2.37438	1.37449	1.68649	/
150-200 (MPa)	2.2848	2.08133	2.15005	/
200-250 (MPa)	4.12297	2.99107	3.08947	/
250-300 (MPa)	9.96002	5.78231	3.09479	/
300-350 (MPa)	/	9.19131	12.30809	/
5.7-40 (MPa) (Ref. 1, 2)	/	/	/	2.2
> 40 (MPa) (Ref. 1)	/	/	/	4.5

Table S3

Table S3. Different grain size exponents p for polycrystalline methane hydrates. The grain size exponent p is estimated from our simulation results for polycrystalline methane hydrates at 263.15 K under a loading stress of 300 MPa.

Grain size (nm)	4-7	7-10	10-13	13-16
grain size exponent p	3.45794	2.08097	0.31907	-0.92318

Table S4**Table S4. Different steady-state creep mechanisms of polycrystalline methane hydrates.**

Superscript *a* refers to the average stress exponent *n* at different ranges of the loading stress, and these average stress exponents *n* can be estimated from the Tables S2-S3 above. Superscript *b* refers to estimates from Table S3.

Main creep mechanisms	grain size exponent <i>p</i>	stress exponent <i>n</i> or loading stress (MPa)	Temperature (K)
Lattice vibration/GB diffusion/ lattice diffusion	$\geq \sim 3.46$	$< \sim 9.96$	263.15
GB diffusion/ GB sliding	~ 2.08	$7.49^a \sim 7.70^a$	263.15
GB diffusion/ GB sliding	~ 0.32	300 MPa	263.15
GB diffusion/ GB sliding	~ -0.92	300 MPa	263.15
Lattice vibration/GB diffusion	$\sim 2.08^b$	$\sim 1.53^a$	263.15
Lattice vibration/GB diffusion	$\sim 2.08^b$	$\sim 2.12^a$	263.15
Lattice vibration/GB diffusion	$\sim 2.08^b$	$\sim 3.04^a$	263.15
GB diffusion/ GB sliding	$\sim 2.08^b$	$\sim 4.44^a$	263.15
GB diffusion/ GB sliding	$\sim 2.08^b$	$\sim 10.75^a$	263.15

References

1. W. B. Durham, S. H. Kirby, L. A. Stern and W. Zhang, *J. Geophys. Res.*, 2003, **108**, 2182.
2. W. B. Durham, L. A. Stern and S. H. Kirby, *Can. J. Phys.*, 2003, **81**, 373-380.